Investigating water vapor variability by ground-based microwave radiometry: evaluation using airborne observations

Stefan Kneifel, Susanne Crewell, *Member, IEEE,* Ulrich Löhnert, and Jan Schween,

***Abstract*—This letter introduces a new approach to characterize small scale humidity variations using ground-based microwave radiometry. For that purpose a microwave profiler routinely performed different scan patterns during its deployment at the ARM mobile Facility in the Black Forest, Germany. Individual azimuth scans at 30° elevation revealed spatial variations in integrated water vapor up to ± 10%. Aircraft observations were used to evaluate the performance of the microwave observations by comparing derived humidity fields with integrated water vapor retrieved along individual directions of the microwave radiometer. Distinct humidity signals were reproduced by both observations. Residual uncertainties can be attributed to the temporal variations during the time it took the aircraft to cover the boundary layer and uncertainties in the interpolation. Longterm scanning observations will be further explored to investigate land surface interaction and to characterize subgrid variability.**

***Index Terms*—Microwave radiometry, atmospheric measurements, remote sensing**

I. Introduction

WATER vapor, the most important greenhouse gas, also plays a crucial role within the hydrological cycle. Its spatial distribution is determined by advection, the processes of evaporation at the surface and cloud forming/dissipation. Their correct description still provides large challenges for today's weather forecast and climate models. The evaluation of such models is typically done by comparing observations at a single site with model grid box values. However, sub-grid variability and horizontal inhomogeneities can introduce an additional uncertainty in such intercomparisons. The knowledge of water vapor variation is also an interesting information in itself since it is connected to land-surface exchange processes, initiation of convection and cloud development. Especially water vapor variations in the boundary layer (BL) influence the development of convective precipitation and are therefore important for quantitative precipitation forecasting [1], [2]. For example, Crook [3] shows using a cloud resolving model that the initiation of deep convection can depend on variations in temperature of 1 K and 1 $kg \cdot m^{-2}$ in the water vapor field within and just above the boundary layer. Even in non convective situations sub-grid variability of clouds is rather important because cloud fraction mainly determines the radiative energy input to the surface. Today's models mostly use relatively simple parametrizations to diagnose cloud fraction from grid-scale humidity. The information about water vapor variation could be valuable to develop/improve statistical cloud schemes which assume probability density functions of water vapor.

Current observational techniques either measure the humidity only at the surface, as vertical columns (Integrated Water Vapor IWV) or profiles. Classical radiosonde profiles and aircraft measurements are representative only for a small part of the atmosphere and their temporal and spatial resolution is coarse. Active lidar techniques e.g. Differential Absorption Lidar (DIAL) reveal the fine 3D-structure of the water vapor field [4] but are currently not suitable for autonomous, continuous operation and are also blocked by the presence of clouds. The observation of the refractivity from S-band radar measurements [5] provides information about the humidity field close to the surface but requires a sufficient number of well known targets. Passive microwave radiometers (MWR) have proven to be valuable tools to derive profiles of temperature, humidity, integrated water vapor content (IWV) and liquid water path (LWP) in nearly all weather conditions and are being operated at several sites world wide in zenith mode. This study demonstrates their potential for continuously monitoring the spatial variability of water vapor using azimuth and elevation scanning. In order to validate the observations, an aircraft intercomparison campaign has been performed.

II. Observations

Observations used in this study were performed within the framework of the Convective and Orographically-induced Precipitation Study (COPS) in 2007 [6]. The scanning Humidity and Temperature Profiler HATPRO [7] was deployed on the roof of the Atmospheric Radiation Measurement Program (ARM) Mobile Facility (AMF) in the Black Forest Murg Valley, Germany (48.32 N, 8.23 E, 511 m

Manuscript received May 31, 2008. This work was supported in part by the German Science Foundation (DFG) under grants WU-356/4-2 and TR32. Aircraft flights for the NEWVAP project were sponsored by EUFAR.

S. Kneifel, S. Crewell, U. Löhnert, J. Schween are with the Institute for Geophysics and Meteorology, University of Cologne, Germany (phone: +49 221-470-1610; fax: +49 221-470-5161; e-mail: skneifel@meteo.uni-koeln.de).

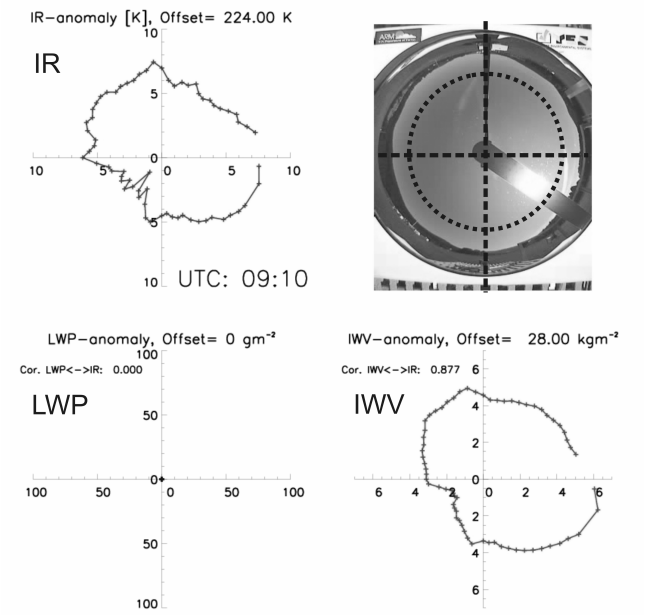

Fig. 1. Azimuth scan at 30° elevation providing IR-temperature [K] (top left), LWP [$g \cdot m^{-2}$] (bottom left) and IWV [$kg \cdot m^{-2}$] (bottom right) together with corresponding sky picture of the Total Sky Imager (TSI, top right) for August 5, 9:10 UTC at the AMF. Data are shown as anomalies from the given offset value. The 30° elevation is denoted in the TSI image by the dotted circle.

ASL). The site was located in the North-South oriented Murg valley which is roughly 1 km wide. Both sides of the valley are covered with forest and elevation increases 280 m towards East and 350 m towards West.

HATPRO is a 14-channel microwave radiometer observing atmospheric emission in two bands. The technical specifications and calibration methods of HATPRO are described in [7]. In this study we focused on the seven channels between 22.235 and 31.4 GHz along the wing of the 22.235 GHz rotational water vapor line. All of these channels were used to derive IWV and LWP via multi-linear regression [7] yielding accuracies better than 0.7 $kg \cdot m^{-2}$ and 20 $g \cdot m^{-2}$ respectively. The antenna half power beam width (HPBW) for the channels along the water vapor line is 3.5° with a side lobe suppression of better than 30 dB. That means that 99.9% of the received power stems from an angle range of ±5.25°. Additionally a Heitronics KT19.85 infrared (IR) thermometer (9.6-11.5 µm) was attached to the MWR. In the measurement range from 223-473 K a resolution of ±0.1 K can be achieved. The accuracy is $\pm 0.5K + 0.007 \cdot |T_h - T_t|$ with T_t being the temperature of the measured target and T_h the temperature of the thermometer housing. Supposed T_h = 300 K and T_t = 223 K (e.g. in case of a blue sky) the accuracy is ±1.0 K. In the wavelength region of 9.6-11.5 µm the atmosphere is nearly transparent with relatively low – however detectable – contributions from water vapor and rather minor contributions from ozone. Since clouds strongly emit infrared radiation the observed IR-temperature is roughly proportional to cloud base temperature in cloudy conditions. In contrast to the MWR the IR is also sensitive to the presence of ice clouds.

Different kinds of automated scan patterns were carried out in order to best characterize atmospheric variability. Elevation scans around ~60 GHz are best suited to derive high accuracy temperature profiles from the boundary layer [8], whereas azimuth scans give the opertunity to investigate the spatial variability of the water vapor and cloud field [9]. From July 6 until August 28 regular azimuth scans of IWV, LWP and IR-temperature with 5° resolution in azimuth at fixed 30° elevation were carried out approx. every 15 minutes. Every azimuth scan (duration ~4.5 minutes) was followed by an elevation scan (~2 minutes); in the remaining time zenith observations were performed with a temporal resolution of one second.

In order to evaluate the potential of the MWR scanning observations, in situ aircraft observations were performed by the motor glider Metair Dimona on July 26 and August 1. These measurements were part of the NEWVAP project (New Methods for characterizing Energy and Water Vapor Exchange Processes) within the EUFAR (European Fleet for Airborne Research) program. Humidity is measured with a Meteolabor dewpoint mirror for reference and a Licor LI7500 open path infrared gas analyser. The LI7500 is mounted outside with its long axis in flight direction. It is surrounded by an open cage to reduce pressure fluctuation due to turbulence. Temperature and pressure are measured within the cage to derive water vapor mixing ratio from the primarily measured water vapor concentration. This sensor configuration allows to measure water vapor mixing ratio with an accuracy of 0.1 $g \cdot kg^{-1}$ and a resolution of 0.05 $g \cdot kg^{-1}$.

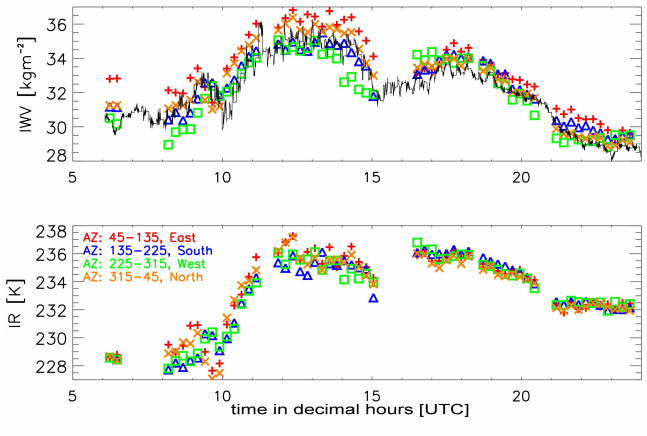

Fig. 2. Temporal development of IWV (top) and IR-temperature (bottom) on August 5 for the four different spatial sectors: East (45-135°, red plus signs), South (135-225°, blue triangles), West (225-315°, green squares) and North (315-45°, yellow crosses). The IWV from zenith looking measurements is shown as thin black line (values are multiplied with a factor two for better comparison with the 30° azimuth scans). No data are available during the night hours when dew contaminated the MWR radome. Data from 7-8 and 15-16 UTC are disregarded because the sun was close to 30° elevation in these periods (sunrise at 4 UTC, sunset at 19 UTC).

TABLE I
STATISTICAL SCAN PROPERTIES DURING CLEAR SKY FOR IWV

Direction	Mean [kg · m^{-2}]	Median [kg · m^{-2}]	STD	%<-1.5 kg · m^{-2}	%>+1.5 kg · m^{-2}
North - East	-0.04	-0.02	0.78	4.2	3.2
North - South	-0.18	-0.15	1.04	10.0	6.0
North – West	-0.09	-0.08	0.70	2.8	1.5
East – West	-0.05	-0.02	0.97	6.3	4.7
East – South	-0.14	-0.12	0.71	2.9	2.2
South - West	+0.09	+0.05	0.84	4.4	4.2

687 scans (LWP <50 g · m^{-2})

III. MEASUREMENTS

A. Scan example for a cloudfree day

When looking at individual azimuth scans, a high spatial variability in the water vapor field can be observed. Approximately 90% of the IWV in the atmosphere is located in the lowest 5 km. Thus, the azimuth scans with 30° elevation basically show the variation of the humidity within a horizontal distance of 9 km from the radiometer. Assuming the tropopause at ~10 km height the maximal horizontal range which contributes to the humidity signal is at ~17 km. To ensure the azimuth scans are not contaminated by the surface the elevation angle of the surrounding orography was measured by theodolites and was found to be everywhere lower than 18°. In this study we concentrate only on clear sky cases to keep the situation as simple as possible. On August 5 a high pressure system over Central and Southern Europe caused strong subsidence and within a weak flow from the South-East warm air was advected over the COPS area. Under these conditions no convective clouds could develop during the day. The significant asymmetric IWV distribution can be seen in the azimuth scan at 09:10 UTC (Fig. 1). The IWV has

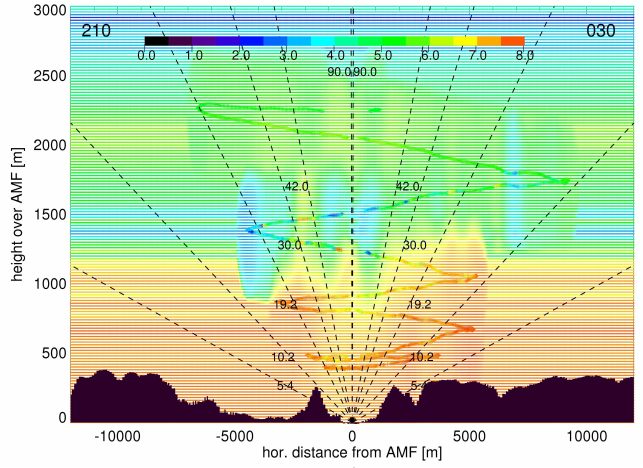

Fig. 3. Water vapor mixing ratio [g · kg^{-1}] (colorbar) along a South-South-West (210°) – North-North-East (30°) transect as a function of height above the AMF site (511 m asl). Thick tracks represent observations by the Metair Dimona performed between 13:04 and 13:38 UTC on July 26. Dashed lines refer to the elevations at which MWR observations were taken. Black regions symbolize the local orography. The underlying humidity field is a combination of interpolated aircraft measurements and the closest AMF-radiosonde (max. 2h difference to measurements).

the highest values in the easterly directions with up to 34 kg · m^{-2} whereas the smallest IWV is located in the South-West with 30 kg · m^{-2} corresponding to a maximal difference of 4 kg · m^{-2} (12%). These values are for the slant path at 30° and need to be divided by two to give zenith equivalent values. The high correlation between IR-temperature and IWV (0.88) independently confirms this asymmetry of the humidity field. The highest temperature of 231.5 K in the IR-scan can be found accordingly in the East. In the South-West where the lowest water vapor was measured, also the coldest sky temperature with 225 K was found. In the absence of clouds the structure of the IR-temperature mainly stems from the distribution of water vapor in the atmosphere. It has to be noted that at these low sky temperatures the IR-thermometer approaches its detection limit of 223 K. Thin contrails which are visible in the sky pictures from the Total Sky Imager (TSI) might also deteriorate the correlation between IWV and IR-temperature.

B. Temporal evolution

For the analysis of the temporal development of IWV, LWP and IR-temperature the azimuth scans were spatially averaged in four sectors, two along the valley (North: 315-45°, South: 135-225°) and two across (West: 225-315°, East: 45-135°). After sunrise at 4 UTC the IWV in all sectors increases by 4-5 kg · m^{-2} (13-16%) during the morning hours (Fig. 2). The azimuth scans from 8 to 15 UTC show a clear asymmetry in the water vapor field. Starting at 10 UTC the IWV is ~2 kg · m^{-2} lower in the South/West than in the North/East. As indicated in Fig. 1, several azimuth scans show maximum differences between individual directions up to 4 kg · m^{-2}. However, the spatial averaging over 90° leads to smaller differences between the individual sectors in Fig. 2. The IWV zenith measurements between the different scans are nearly the mean of the four sector values when multiplied with the airmass factor of two for 30° elevation (Fig. 2). The stronger turbulence during the day (10-18 UTC) is clearly visible in the increased variability of the zenith IWV. The temporal evolution of the IR-temperature is similar to the IWV with higher spatial variability during daytime (1-2 K). However, spatial differences are more difficult to identify, probably due to contrails, which could be observed with the TSI.

C. Statistical Evaluation

All cloud-free (LWP < 50 g · m^{-2}) azimuth scans from the two month period were statistically analysed. To investigate systematic structures in the distribution of IWV the mean differences of the four azimuth sectors were calculated (Table 1). The mean differences are not disturbed by possible systematic errors (e.g. calibration errors) because they would equally appear in every azimuth direction. The high number of 687 scans with 18 measurements per azimuth sector strongly reduces the influence of radiometer noise or retrieval based uncertainities on the statistical analysis. The largest mean differences occur in North-South with -0.18 kg · m^{-2} and in East-South with -0.14 kg · m^{-2}. This indicates that the

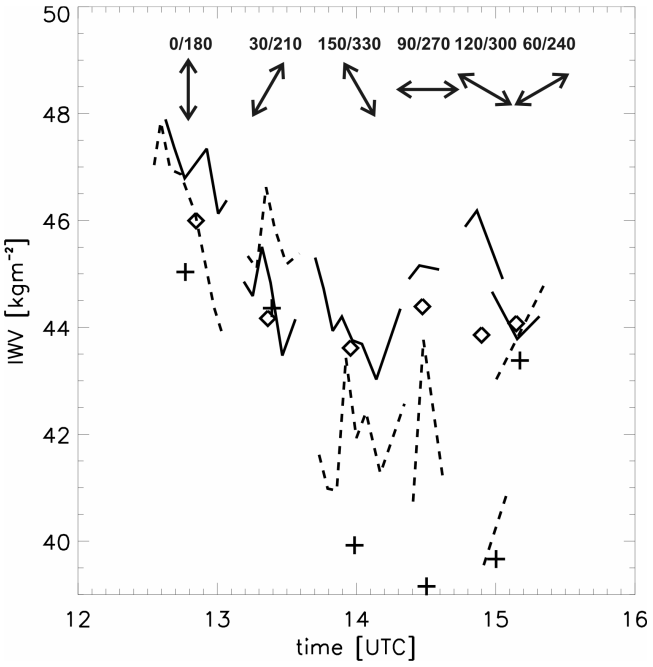

Fig. 4. Temporal development of IWV during the aircraft flights on July 26. Lines show the temporal evolution of the 30°-IWV measured by HATPRO elevation scans (10s temporal averaging for each elevation angle) in the current flight direction which is illustrated by the double-headed arrows above. The deduced IWV values from the interpolated humidity fields are plotted as symbols. The eastern azimuth directions (0-150°) are shown as solid lines/diamonds and the western azimuth directions (180-330°) are drawn as dashed lines/plus signs.

atmosphere is slightly more humid in the South compared to the North and East. The largest spatial variation (standard deviation STD) of the IWV difference is 1.04 $kg \cdot m^{-2}$ in North-South and 0.97 $kg \cdot m^{-2}$ in East-West. However, the spatial IWV differences are not equally distributed. Especially in the South 10% of all scans are more than 1.5 $kg \cdot m^{-2}$ moister when compared to the North. These IWV distributions can be caused by local circulations within the boundary layer as well as by synoptic processes. Thus, in further studies an enlarged dataset should be analyzed for different weather classifications and in combination with other sensors.

IV. Aircraft Intercomparison

The aircraft measurements were performed to investigate the potential of a passive microwave profiler for the detection of the spatial variability of water vapor in the troposphere. For that purpose the Metair-Dimona mapped the water vapor within the Murg Valley. The flight pattern was star like with 6 vertical planes spaced by 30° in azimuth angle. The first plane was flown in N-S (0-180°), the second in NNE-SSW (30-210°) and so on (illustrated by the double-headed arrows in the top part of Fig. 4). In each azimuth plane the aircraft was descending (or ascending) from around 1500 m to 50 m above ground. At the same time HATPRO performed synchronous elevation scans in the azimuth planes and in between some azimuth scans to observe both the temporal and spatial

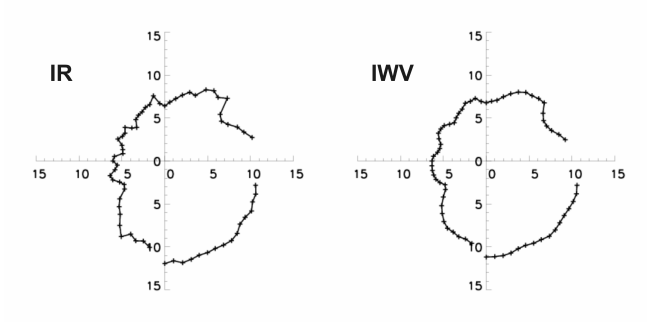

Fig. 5. Azimuth scan (30° elevation) on July 26 at 13:56 UTC measured at the AMF site showing IR temperature-225 K (left) and IWV-35 $kg \cdot m^{-2}$ (right).

variability. The observation geometry is illustrated in Fig. 3 for a cross section from SSW (210°) to NNE (30°) which took about 30 min for the aircraft to complete.

The aircraft data were interpolated from the flight path into the azimuth plane in order to construct 2D humidity and temperature fields. These fields allow to 1) compute IWV along HATPRO's slant paths and 2) perform radiative transfer simulations for comparison with the observed brightness temperatures. Therefore a 2D-grid was generated with maximum dimensions of 260 km in the horizontal and 24 km in the vertical direction. The long horizontal distance is necessary since HATPRO's lowest elevation angle of 5.4° reaches the upper boundary at that distance. The HATPRO measurements from the lowest elevation angle could only be used in the north direction because in the other directions they were blocked by orography. Nevertheless, all interpolated fields were generated with the same horizontal extent. The vertical dimension is necessary for realistic radiative transfer simulations.

The 2D-grid has a horizontal resolution of 50 m in close distance (0 to 12 km) from the AMF and a 500 m resolution at farther distances. In the vertical direction the resolution is 20 m in heights up to 3 km and 200 m in the region above from 3.2-24 km. The grid was first filled with the mean vertical humidity profile of aircraft measurements combined with the closest radiosounding (max. 2 hours difference to measurements). In regions where aircraft measurements were available, the field was corrected by this data. The measurements were interpolated onto the grid with a distance dependent weighting function w_i. For this the distance d_i of each aircraft measurement point q_i within the cutoff radius r_{max} = 500 m around the grid point $q_{gr}(x,z)$ was calculated.

$$w_i = \frac{r_{\max}^2 - d_i^2}{r_{\max}^2 + d_i^2} \quad (1)$$

To avoid strong gradients on the boundary of the interpolated field the mean humidity profile $q_{mp}(z)$ was added as a further measurement point in the interpolation routine:

$$q_{gr}(x,z) = \frac{\sum_{i=1}^{n}(w_i \cdot q_i) + w_{mp} \cdot q_{mp}(z)}{\sum_{i=1}^{n} w_i + w_{mp}} \quad (2)$$

Here n is the total number of aircraft measurements within the cutoff radius. In the weighting function w_{mp} for the mean profile d_i is replaced by d_{mp} which is defined as

$$d_{mp} = r_{\max} - \frac{1}{n}\sum_{i=1}^{n} d_i \qquad (3)$$

This definition of d_{mp} accounts for the mean distance of the measurements to the grid point. That means that the closer the measurements are to the grid point the smaller is the contribution of the mean profile and vice versa.

The interpolated humidity fields were then used to derive the IWV at different elevation angles according to the angles used in the HATPRO elevation scans. The data from July 26 (Fig. 3) reveal strong variations in IWV in a well developed boundary layer with dry convection and no clouds. The weather in the COPS region on this day was dominated by advection of warm air from South-West and strong subsidence caused by an intensifying high pressure system over Southern and Central Europe. This situation inhibited the development of convective clouds during the whole day.

A comparison of the MWR-retrieved IWV at 30° elevation with the deduced IWV from the interpolated humidity field is shown in Fig. 4. If the real atmosphere were accurately represented by the interpolated humidity field the deduced IWV should be the temporal mean of the HATPRO measurements in each azimuth direction. Due to the limited coverage of the aircraft measurements the IWV deduced from the interpolation field differs from the temporal mean of the MWR measurements by up to 2 $kg \cdot m^{-2}$ - especially in those azimuth directions where the aircraft only flew short legs. However, the strong decrease of 4-7 $kg \cdot m^{-2}$ in IWV from 12-14 UTC as well as the strong difference between the complementary azimuth directions in the East-West direction are evident in both data sets. Additionally the HATPRO measurements show a strong temporal variability in IWV at one and the same observation angle. For example, the IWV in the South (180°) decreases from 48 $kg \cdot m^{-2}$ to 44 $kg \cdot m^{-2}$ within only 30 minutes. Looking at the azimuth scan with 30° elevation from 13:36 UTC (Fig. 5) as a spatial 'snapshot' of the humidity field the strong drying of the atmosphere in the northwestern direction can be observed both in the IWV and IR-temperature. The difference from Northwest to Southeast in the IR-temperature is about 6 K and 4 $kg \cdot m^{-2}$ in the IWV. The elevation scan and the IWV from the interpolated field in the azimuth plane 150/330 (Fig. 4) measured shortly after the azimuth scan show similar differences of 3.5 $kg \cdot m^{-2}$ with strong temporal variations. In summary the results from HATPRO's different scan modi show good structural agreement with the aircraft-derived interpolated humidity fields, even though these cannot completely represent the atmosphere.

V. Conclusion

We have demonstrated the potential of scanning microwave observations to continuously monitor the spatial variability of water vapor. Remarkable fluctuations of the water vapor field could be observed even in cloud free scenes on several days. Airborne observations are well suited to resolve strong spatial variations in humidity which cannot be resolved by passive profiling systems. However, aircraft measurements cannot resolve temporal changes well, which we have shown to be well captured by scanning MWR measurements in terms of path-integrated IWV. Such observations can be helpful for e.g. characterization of land-surface exchange of humidity, subgrid variability and investigation of convective initiation.

From September to December 2007 the radiometer performed volume scans with 10° by 10° resolution. Due to reduced integration time these scans took about 10 min. These data will be used to extend our analysis to the full hemisphere. In addition to water vapor, HATPRO can simultaneously determine the liquid water path along the observed slant path. The interpretation of such measurements however, is more difficult as it is not obvious how the beam passes through the cloud. Further analysis will therefore focus on the interpretation of hemispheric LWP and its connection to the water vapor field. Herein the AMF data set including TSI, cloud radar and lidar will be important to better interpret the scanning data.

Acknowledgment

We thank the ARM program for providing data and the site technicians for supporting the deployment of the microwave radiometer HATPRO at the ARM Mobile Facility.

References

[1] Weckwerth et al., "An overview of the International H2O Project (IHOP_2002) and some preliminary highlights." *Bull. Amer. Meteor. Soc.*, vol. 85, pp. 235-277, 2004.

[2] F. Fabry, „The Spatial Variability of Moisture in the Boundary Layer and Its Effect on Convection Initiation: Project-Long Characterization." *Monthly Weather Review*, vol. 134, pp. 79–91, 2006.

[3] N. A. Crook, "Sensitivity of moist convection forced by boundary layer processes to low-level thermodynamic fields." *Monthly Weather Review*, vol. 124, pp. 1767-1785, 1996.

[4] Wulfmeyer et al., "Four-dimensional variational assimilation of water vapor differential absorption lidar data: The first case study within IHOP_2002." *Monthly Weather Review*, vol. 134, pp. 209-230, 2006.

[5] Fabry, F., C. Frush, I. Zawadzki, and A. Kilambi, "On the extraction of near-surface index of refraction using radar phase measurements from ground targets." *J. Atmos. Oceanic Technol.*, vol. 14, pp. 978-987, 1997.

[6] Wulfmeyer et al., "The Convective and Orographically-induced Precipitation Study: A research and development project of the World Weather Research Program for improving Quantitative Precipitation Forecasting in low-mountain regions." *Bull. Amer. Meteor. Soc.*, June 2008, accepted.

[7] Rose, T., S. Crewell, U. Löhnert, and C. Simmer,"A network suitable microwave radiometer for operational monitoring of the cloudy atmosphere." *Atmos. Res*., vol. 75, no. 3, pp. 183-200, 2005.

[8] Crewell, S., and U. Löhnert, "Accuracy of boundary layer temperature profiles retrieved with multi-frequency, multi-angle microwave radiometry." *IEEE Trans. Geosci. Remote Sens.*, vol. 45, no. 7, pp. 2195-2201, 2007.

[9] Martin, L., M. Schneebeli, and C. Mätzler, "Tropospheric water and temperature retrieval for ASMUWARA.", *Met. Z.*, vol. 15, no.1, pp. 37-44, 2006.